Deliyannis, Theodore L. et al "Realization of High-Order Functions"
Continuous-Time Active Filter Design
Boca Raton: CRC Press LLC,1999

Chapter 5

Realization of High-Order Functions

5.1 Introduction

In most cases, the selectivity provided by a second-order filter is not adequate. Higher-order filter functions have to be realized in order to satisfy the stringent selectivity requirements in telecommunication systems, special instrumentation, and many other applications.

To realize such high-order filter functions, two main approaches have been found most useful in practice. The first is to cascade second-order stages without feedback (cascade filter) or through the application of negative feedback (multiple-loop feedback filters, MLFs). The second is to use combinations of active (e.g., opamps) and passive (resistors and capacitors) components in order to simulate either the inductances or the operation of a high-order LC ladder. Yet another approach, the use of just one opamp embedded in an RC network in order to realize the high-order function, although possible, has been dropped for reasons of high sensitivity.

The study of such high-order circuits requires some additional tools over those used in the previous chapter, which were suitable for second-order filters. For example, in an MLF or a simulated ladder filter, the value of each component does not affect only one pole or one zero of the filter, but more than one, making thus the filter tuning difficult. In this case, the Q sensitivity for, example, of a biquadratic section in the MLF circuit cannot be used as a criterion when comparing the MLF circuit to the simulated ladder. Therefore, more suitable sensitivity measures are required for such comparisons, the determination of which makes the use of a computer program unavoidable.

In this chapter, we first discuss briefly a number of criteria which characterize a useful, practical, active RC filter. Next, we introduce suitable sensitivity measures, which have been proven to be consistent with one another, as far as the information on sensitivity they give is concerned. Then, three high-order filters are discussed, all of them using the biquadratic circuit as a cell. These are the cascade, the multiple-loop feedback, and the cascade of biquartic stages filters, the latter being a mixture of the other two. The simulated LC ladder filter is examined in the next chapters.

5.2 Selection Criteria for High-Order Function Realizations

The realization of a high-order function can be achieved by a number of methods. Some of these have proved more advantageous in practice than others, and over the years they have

prevailed. Before we see which methods are more acceptable in practice and therefore more useful in filter design, we should set a number of criteria that a design method must satisfy in order to be considered more suitable than others in solving a design problem. It must be emphasized, though, that there is not one method that is the best according to all criteria. So, we will consider the best method as the one that satisfies most of the criteria in a more satisfactory way than the rest.

The most important criteria that can be used in comparing the various methods of realization of a high-order function are the following:

- The possibility of realizing the required function using the available components.
- Sensitivity, i.e., stability of the filter characteristics. As we have already seen in the previous chapter, some biquads are more sensitive than others to variations in their component values. This is also true in high-order circuits.
- Economy. Some design methods lead to circuits that require fewer components than others and therefore are more advantageous from the economy point of view.
- Simplicity of design. The designer prefers to use an easy to understand and apply design method rather than a more complicated one.
- The possibility of producing the filter in integrated circuit form. Of course, this will depend on the number of filters to be manufactured; otherwise it will not be economical.
- Power dissipation. Lower power dissipation relaxes the power supply design and leads to lower heat produced by the filter.
- Tuning simplicity. Every circuit, after it has been built, requires tuning in order to satisfy the required specifications.
- Dynamic range. This determines the range between highest signal level that will pass undistorted through the filter and the lowest signal that can be distinguished from the noise. This is usually expressed in decibels and may be written as

$$\Delta R = \frac{\text{Maximum signal level}}{\text{Minimum signal level}} = \frac{\text{Distortion limit}}{\text{Noise floor}}$$

- Noise. Active elements produce their own noise, which is added to that of the passive components, thus decreasing the signal-to-noise ratio at the output of the filter.
- Other criteria, such as passband attenuation, etc., that the designer may set as applicable in the specific filter design problem.

Clearly, some of these criteria cannot be satisfied by the same circuit. For example, low sensitivity and small number of opamps (economy) used in the circuit cannot be satisfied simultaneously, as we have already seen in the realization of second-order functions. Also, a low-sensitivity circuit that employs a large number of opamps dissipates higher levels of dc power and produces more noise than other, more sensitive circuits that use a lower number of opamps. Thus, the task of the designer is to select a circuit design that satisfies most of the criteria that are considered more important for the filter design problem at hand.

5.3 Multiparameter Sensitivity

In the previous chapter (Section 4.4), we introduced various sensitivity measures useful in the case of the realization of second-order functions. These measures of sensitivity can, in some cases, be of some importance when studying the sensitivity of a high-order filter, too. However, they do not give a complete picture of the sensitivity of such a filter, due to the large number of its components.

More useful in sensitivity studies of high-order filters have been proved to be the so-called multiparameter sensitivity measures. Some of these are reviewed here below:

1. Worst-case sensitivity *WS* defined as follows:

$$WS = \sum_{i=1}^{n} \left| S_{xi}^{|H|} \right| \tag{5.1}$$

   where n is the number of elements, passive and active, and H the filter transfer function.

   Since H is a function of ω too, WS, is also a function of frequency. Worst-case sensitivity estimates the worst deviation from the nominal response when all components have the same percentage variation.
2. Schoeffler's sensitivity measure, in its simplified form, is defined as follows [1]:

$$\sigma_{\Delta|H|/|H|}^2 = \sigma^2 \sum_i \left| S_{xi}^{H} \right|^2 \tag{5.2}$$

   where $\sigma_{\Delta|H|/|H|}$ is the standard deviation of $|H|$, and σ the standard deviation of resistors and capacitors, assumed to be the same for all these components, with the additional requirement that they are uncorrelated.

   Both these multiparameter sensitivity measures require for their determination the calculation of $\partial|H|/\partial x$ for all x_i, assuming they vary independently. However, since the variations of the components, in practice, are not infinitesimal, a more realistic picture, and therefore, more useful in engineering work, would be a sensitivity measure based on the real type of component variations, as is the following one.
3. Standard deviation of the amplitude response for a large number of measurements. Here, as a measurement, we consider the calculation of the amplitude response using one set of component values that have been obtained at random within the tolerance limits of the components. In doing this, we assume that the component values have a uniform or normal distribution around its nominal value. The limits of the distribution are set by the tolerance of the components.

   The standard deviation $\sigma_{\Delta|H|/|H|}$ is determined using the following formula [2]:

$$\sigma_{\Delta|H|/|H|}^2 = \frac{1}{N} \sum_{i=1}^{N} |H_i|^2 - \left(\frac{1}{N} \sum_{i=1}^{N} |H_i| \right)^2 \tag{5.3}$$

or by the formula for a smaller number of measurements

$$\sigma^2_{\Delta|H|/|H|} = \frac{1}{N-1}\sum_{i=1}^{N}|H_i|^2 - \frac{1}{N(N-1)}\left[\sum_{i=1}^{N}|H_i|\right]^2 \tag{5.4}$$

where N, the number of measurements, is

$$100 < N < 10{,}000$$

Since $|H_i|$ is a function of ω, so is $\sigma_{\Delta|H|/|H|}$.

The component random values can be obtained as follows: the computer is instructed to give each time two random numbers, r_1 and r_2, both between 0 and 1. Assuming a uniform distribution of component values around the nominal value, if δ_x is the tolerance of the component with nominal value x, its random value x' will be either

$$\begin{aligned} x' &= x(1+\delta_x r_1) \quad \text{if } r_2 \le 0.5 \\ x' &= x(1-\delta_x r_1) \quad \text{if } r_2 > 0.5 \end{aligned} \tag{5.5}$$

The standard deviation multiparameter sensitivity measure is used in comparing high-order circuits realizing the same filter function below. However, use of the other two measures leads to similar conclusions; therefore, they can also be applied in multiparameter sensitivity calculations.

5.4 High-Order Function Realization Methods

The most useful methods for the realization of high-order filter functions in practice fall into one of the following three general methods:

1. Cascade connection of second-order sections
2. Multiple-loop feedback circuits
3. Simulation of passive LC ladder networks

In Method 1, taking advantage of the useful biquadratic sections we examined in the previous chapter, we write the high-order function as the product of biquadratic factors that we realize accordingly. Next, we cascade these sections by connecting the output of each section to the input of the following one. This method has the advantages of simplicity in designing and aligning the filter, provided that the output of each section is of very low impedance—practically zero.

In Method 2, multiple feedback and, in some cases, multiple feed-forward is applied in a cascade connection of biquadratic sections. This coupling, as we shall see later, leads to a better sensitivity performance of the overall circuit compared to the corresponding circuit obtained by Method 1.

Simulation of passive resistively-terminated lossless ladder networks can be achieved by simulating either the inductances of the ladder, using GICs, PICs, gyrators, or functionally.

Functional simulation here implies that branch currents and node voltages in the ladder are modeled using analog computer simulation techniques. The ladder simulation method is attractive, because it leads to active circuits of lower sensitivities than the other two methods.

For simplicity reasons in design and filter alignment, a combination of Methods 1 and 2 may, in some cases, lead to useful circuits having the advantages of both methods. According to this method, the high-order function is written as the product of biquartics (fourth-order functions), which are realized as multiple-loop feedback sections and then cascaded.

In this chapter, Methods 1 and 2, as well as their combination, i.e., the cascade of biquartic sections, are explained to some detail. As previously mentioned, the simulation of resistively terminated ladder lossless filters is explained in following chapters.

5.5 Cascade Connection of Second-Order Sections

A high-order filter function $T(s)$ [we shall use $T(s)$ here for notational simplicity] can be realized as the ratio of the output voltage to the input voltage of a cascade connection of lower-order stages, each of which does not load the output of its preceding one. For this to be true, the output impedance of each section must be much lower than the input impedance of the following section at all frequencies of interest.

The lower-order stages are preferably biquadratic. Their realization has been presented in the previous chapter. If the function under realization is of odd order, there will be a first-order term which, according to the type of $T(s)$ (lowpass, highpass, or allpass), can be realized by one of the first-order circuits suggested in Chapter 4.

Thus, the high-order filter function $T(s)$ will be written in the form

$$T(s) = t(s) \cdot \prod_{i=1}^{N} t_i(s) \tag{5.6}$$

where $t(s)$ is a first-order term, or simply unity, depending on the order n of the function, which is either odd ($n = 2N + 1$) or even $n = 2N$, respectively, with N being an integer and

$$t_i(s) = \frac{a_{i2}s^2 + a_{i1}s + a_{i0}}{s^2 + b_{i1}s + b_{i0}} \tag{5.7}$$

Depending on $T(s)$, one or two of the numerator coefficients in Eq.(5.7) may be zero, while in the case of an allpass function, the numerator coefficients will be equal to the corresponding coefficients of the denominator, with the additional constraint that $a_{i1} = -b_{i1}$, with $b_{i1} > 0$.

In forming each biquadratic term $t_i(s)$ and then cascading the biquad sections to obtain the overall circuit realizing $T(s)$, three degrees of freedom are at the designer's disposal. These are the following:

- Pole-zero pairing, i.e., which poles with which zeros of $T(s)$ will be paired to form each $t_i(s)$.
- Distribution of the overall gain in the various biquadratics.
- Physical position of each biquad in the cascade.

Clearly, the pole-zero pairing greatly affects the dynamic range of the corresponding biquad and consequently that of the whole filter. Also, the distribution of the filter gain among the various biquads influences their dynamic range, while the biquad sequence in the cascade has a significant effect on the total noise generation in the filter.

Consequently, the filter designer should take advantage of these degrees of freedom in order to optimize the design with regard to the following two main criteria:

- Maximization of dynamic range
- Maximization of the signal-to-noise ratio

In what follows, the optimization approach is explained to some detail with regard to the dynamic range of the filter, which has been shown to be the most relevant [3] in this case.

For reasons of clarity, we give here the universally acceptable definition of the dynamic range of a circuit. It is the ratio, expressed in decibels, of the maximum input signal (voltage) level V_{imax}, that passes undistorted through the circuit to the minimum input signal level V_{imin}, for which the signal at the output of the circuit is still above the output noise level. If the highest output voltage capability for undistorted operation is $V_{o,max}$ and K is the filter gain then the highest input voltage $V_{i,max}$ can be

$$V_{i,\,max} = \frac{V_{o,\,max}}{K} \tag{5.8}$$

Other less important points that may influence the designer's decisions could be the following:

- Minimization of the transmission sensitivity
- Minimization of the passband attenuation
- Simplification of tuning procedure

5.5.1 Pole-Zero Pairing

It will be noted that a complex pole near the $j\omega$-axis creates an elevation in the magnitude response of the corresponding biquadratic term, at frequencies around the imaginary part of the pole. On the other hand, a zero at a similar position creates a deep notch in the magnitude response at frequencies around the imaginary part of the zero. If such a pole and zero are very much apart in the s-plane, and they are paired to form a biquadratic function, the minimum value in the magnitude response inside the passband will be much lower than the maximum value, whether this is inside or outside the passband. In such a case, the input signal level cannot be very high in order to avoid nonlinear operation, and it can not be very low either, because then the signal at the output will be buried in noise at frequencies near the zero.

To avoid such a situation, the magnitude of the biquadratic response should be as flat as possible. To make this more clear, suppose that the magnitude response of the biquadratic term $t_i(j\omega)$ is as shown in Fig. 5.1. Let ω_L and ω_H be the filter passband edges, lower and upper, respectively. What we actually seek with the proper pole-zero pairing is to make the difference between the maximum value $|t_i|_{max}$ wherever in the response, and the minimum value $|t_i|_{min}$ inside the passband as small as possible. To achieve this, we should pair each complex pole with its nearest complex zero.

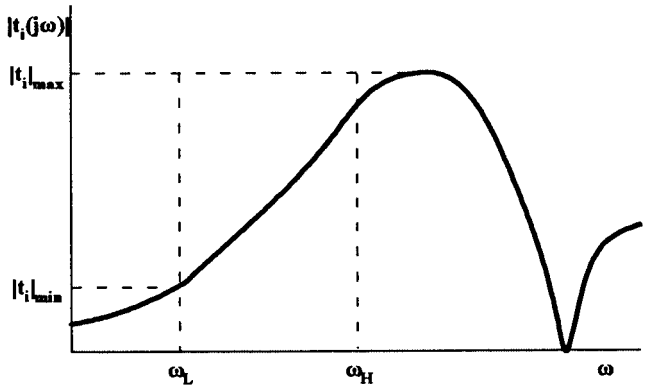

FIGURE 5.1
Biquadratic term.

This argument leads us to the following rule of thumb: to decompose a high-order filter function to the product of biquadratics for maximizing the dynamic range of each biquad (and consequently of the whole filter), we should pair each complex pole with its nearest zero, starting with the pole of highest Q factor.

As an example of the application of this rule, consider the pole-zero positions in Fig. 5.2. (The conjugate poles and zeros are supposed to be placed in the third quadrant). According to the rule of thumb, pole p_1 should be paired with zero z_1, pole p_2 with zero z_2, and pole p_3 with zero z_3. Based on the above argument, a certain algorithm has been suggested by Lueder [4] and discussed by Moschytz [3] for obtaining the optimum pole-zero pairing. The decomposition obtained using the rule of thumb in most cases is identical to the optimum decomposition. When it is not, the degradation in the dynamic range is not substantially different. For this reason, we do not explain the optimum decomposition algorithm here, but we advise the interested reader to consult the above-mentioned references as well as Reference 5.

There are cases, however, when the decomposition can be obtained on a different basis. Consider for example the following sixth-order bandpass function:

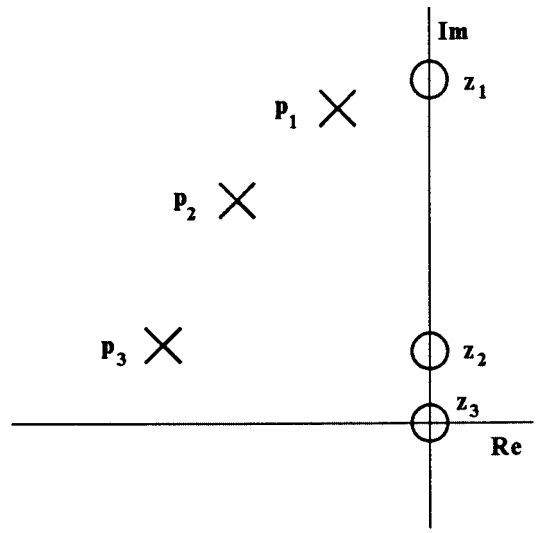

FIGURE 5.2
Illustration of pole-zero positions.

$$T(s) = K\frac{s^3}{(s^2 + b_{11}s + b_{01})(s^2 + b_{12}s + b_{02})(s^2 + b_{13}s + b_{03})} \tag{5.9}$$

Here, all zeros are at zero and infinity. Neglecting at present the distribution of the gain to the three stages, one may decompose $T(s)$ in the following way:

$$T(s) = K\frac{1}{s^2 + b_{11}s + b_{01}} \times \frac{s^2}{s^2 + b_{12}s + b_{02}} \times \frac{s}{s^2 + b_{13}s + b_{03}} \tag{5.10}$$

However, the following decomposition is also possible

$$T(s) = K \cdot t_1(s) \cdot t_2(s) \cdot t_3(s) \tag{5.11}$$

with

$$t_i(s) = \frac{s}{s^2 + b_{1i}s + b_{0i}} \tag{5.12}$$

Each of these two decompositions has practical advantages, and the designer may like to base the pole-zero pairing on these. For example, the lowpass (or the bandpass) section, if placed at the beginning in the cascade, will attenuate out-of-band high-frequency signals, which may otherwise lead to nonlinear operation of the opamps in the subsequent stages. On the other hand, the designer may choose the pole-zero pairing of Eq. (5.11), since a bandpass biquad is easier to tune than the lowpass and highpass configurations.

5.5.2 Cascade Sequence

The proper sequence of the biquads in the cascade is important for achieving maximum dynamic range in the cascade realization of a high-order filter. However, the determination of the best sequence may become a rather tedious procedure if the number of biquads to be cascaded is high. This is so because, for N biquads, there exist $N!$ different sequence possibilities, which will have to be examined.

An efficient algorithm has been described in the literature [6], but we will not explain it here. Fortunately, there exists a simple guide arising from experience that can help the designer to achieve a satisfactory result in practice much easier and quicker.

Thus, we start by determining the frequency of maximum magnitude in each biquad and then form the sequence in such a way that neighboring biquads have their frequencies of maxima as far apart as possible. If there is a lowpass or bandpass section, this is preferably placed in front, while if there exists a highpass, this is placed last. A bandpass section can also be placed last in the cascade, its action being similar to the highpass, namely to prevent any low-frequency noise generated by the leading stages inside the filter from appearing at the output.

A satisfactory solution can also be achieved if the biquads are placed in the cascade in increasing Q factor. It is interesting to note that these mostly intuitive suggestions may help the pole-zero pairing in cases like the example in the previous subsection. Thus, if we select to decompose the sixth-order bandpass function (with all zeros at the origin and infinity) in a lowpass, bandpass, and highpass biquadratics, we associate the lowest Q poles with

the lowpass function, the highest Q poles with the highpass, and the bandpass is left to be associated with the intermediate Q poles. Then, the proper sequence will be the lowpass biquad in front, followed by the bandpass, with the highpass last in the cascade.

Of course, if we had chosen to decompose this sixth-order bandpass function in three bandpass biquadratics, the proper sequence would be in order of increasing Q factor.

5.5.3 Gain Distribution [5]

Having optimized the pole-zero pairing and the biquad sequence in the cascade, we now turn to the distribution of the overall filter gain to the various stages to obtain as high a dynamic range as possible. We consider the filter transfer function of order $2N$ written as follows:

$$T(s) = \prod_{i-1}^{N} k_i t_i(s) \tag{5.13}$$

where $k_1 \cdot k_2 \ldots k_N = K$, with K being the overall gain of the filter and k_i the gain of the ith stage. Let also the biquad sequence be $k_1 t_1(s)$, $k_2 t_2(s)$, $\ldots k_N t_N(s)$.

We work here on the following idea: for the maximum input voltage that results in undistorted output voltage V_o of the filter, the output voltages of the intermediate stages should also be undistorted. To achieve this, we distribute the overall filter gain to the various stages in such a way that the maximum voltage at the output of each intermediate stage is also V_o, i.e.,

$$\max|V_{oi}(j\omega)| = \max|V_{oN}(j\omega)| = V_o \qquad i = 1, 2, \ldots, N-1$$

Let

$$T_i(s) = \prod_{\ell=1}^{i} k_\ell t_\ell(s) \qquad i = 1, 2, \ldots, N-1 \tag{5.14}$$

where $T_i(s)$ is the transfer function from the filter input to the output of the ith stage. Also let

$$\max\left|\prod_{i=1}^{N} t_i(j\omega)\right| = M_N \tag{5.15}$$

and

$$\max\left|\prod_{\ell=1}^{i} t_\ell(j\omega)\right| = M_i \qquad i = 1, 2, \ldots, N-1 \tag{5.16}$$

Then, the gain distribution should be such that

$$k_1 M_1 = K M_N$$
$$k_2 k_1 M_2 = K M_N$$
$$\ldots\ldots\ldots\ldots\ldots\ldots$$
$$\ldots\ldots\ldots\ldots\ldots\ldots\ldots\ldots$$
$$k_{N-1} k_{N-2} \ldots k_1 M_{N-1} = K M_N$$

From these equations, we obtain the following values for all k_j:

$$k_1 = K \frac{M_N}{M_1} \tag{5.17}$$

$$k_2 = \frac{M_1}{M_2} \tag{5.18}$$

and in general,

$$k_j = \frac{M_{j-1}}{M_j} \qquad j = 2, 3, \ldots, N \tag{5.19}$$

where

$$k_N = \frac{K}{\prod_{j=1}^{N-1} k_j} \tag{5.20}$$

As an example, let us design a bandpass filter having a center frequency at 1 krad/s and bandwidth 100rad/s, consistent with the Butterworth response of sixth-order.

Starting with the third-order Butterworth lowpass function,

$$t(s_n) = \frac{1}{s_n^3 + 2s_n^2 + 2s_n + 1} \tag{5.21}$$

we apply the lowpass-to-bandpass transformation

$$s_n = \frac{s^2 + 1}{0.1s}$$

to the lowpass function and obtain the following bandpass function:

$$T(s) = \frac{0.001s^3}{s^6 + 0.2s^5 + 3.02s^4 + 0.401s^3 + 3.02s^2 + 0.2s + 1} \tag{5.22}$$

If we choose to decompose $T(s)$ into three second-order bandpass functions, we will get, from (5.22)

$$T(s) = T_a(s) \cdot T_b(s) \cdot T_c(s)$$

where

$$T_a(s) = k_1 t_1(s) = \frac{k_1 s}{s^2 + 0.1s + 1}$$

$$T_b(s) = k_2 t_2(s) = \frac{k_2 s}{s^2 + 0.0478362s + 0.9170415}$$

$$T_c(s) = k_3 t_3(s) = \frac{k_3 s}{s^2 + 0.0521638s + 1.0904632}$$

with $K = 0.001$ and Q factors $Q_1 = 10$, $Q_2 = 20.02$, $Q_3 = 20.02$.

Having decided on the pole zero pairing, we now turn to the problem of the sequence in the cascade. We have the following possibilities:

$$T_a \cdot T_b \cdot T_c, \quad T_a \cdot T_c \cdot T_b, \quad T_b \cdot T_c \cdot T_a, \quad T_b \cdot T_a \cdot T_c, \quad T_c \cdot T_a \cdot T_b, \quad T_c \cdot T_b \cdot T_a$$

If we choose to follow the rule of thumb for forming the sequence in the order of increasing Q, then T_a should be in front, followed by either T_b or T_c, since T_b and T_c have equal Q factors. We choose the sequence T_a, T_b, T_c.

Next, we have to determine the gain distribution in such a way that the overall gain at the center frequency is unity, i.e., $K = 0.001$. Following the procedure outlined above, we find successively

$$k_1 = \frac{\max|T(j\omega)|}{\max|t_1(j\omega)|} = \frac{1}{10} = 0.1$$

$$k_2 = \frac{\max|t_1(j\omega)|}{\max|t_1(j\omega) \cdot t_2(j\omega)|} = \frac{10}{162.936} = 0.0613738$$

$$k_3 = \frac{K}{k_1 k_2} = \frac{0.001}{0.1 \times 0.0613738} = 0.162936$$

Thus, the final decomposition of the overall bandpass function will be as follows:

$$T_a = \frac{0.1s}{s^2 + 0.1s + 1} \tag{5.23}$$

$$T_b = \frac{0.0613738s}{s^2 + 0.0478362s + 0.9170415} \tag{5.24}$$

$$T_c = \frac{0.162936s}{s^2 + 0.0521638s + 1.0904632} \tag{5.25}$$

Each of these functions will be realized by the SAB shown in Fig. 5.3 and placed in the cascade in the order given in Fig. 5.4.

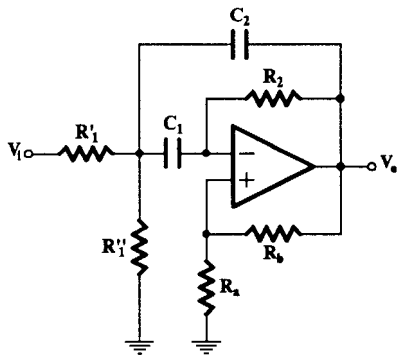

FIGURE 5.3
SAB.

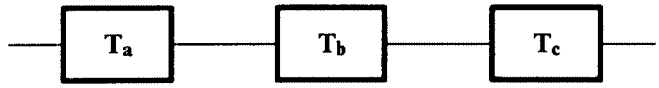

FIGURE 5.4
Cascade sequence.

Following the procedure outlined in Section 4.5, the normalized and denormalized component values ($\omega_o = 1$krad/s, $R_o = 10$ kΩ) are calculated. They are given on Table 5.1.

TABLE 5.1
Component Values

	Section T_1		Section T_2		Section T_3	
Component	**Normalized**	**Denormalized**	**Normalized**	**Denormalized**	**Normalized**	**Denormalized**
		kΩ, nF		**kΩ, nF**		**kΩ, nF**
R'_1	10.27	102.7	16.84	168.4	6.344	63.44
R''_1	0.145	1.45	0.1505	1.505	0.1398	1.40
R_2	7	70	7.3098	73.1	6.70336	67.03
C_1	1	100	1	100	1	100
C_2	1	100	1	100	1	100
R_a	0.265	2.65	0.3368	3.37	0.3368	3.37
R_b	10	10	100	100	10	100

5.6 Multiple-Loop Feedback Filters

We are concerned here with the application of negative feedback in a cascade connection of low-order sections. Two general topologies have been studied extensively:

- The leapfrog topology shown in Fig. 5.5
- The summed-feedback shown in Fig. 5.6

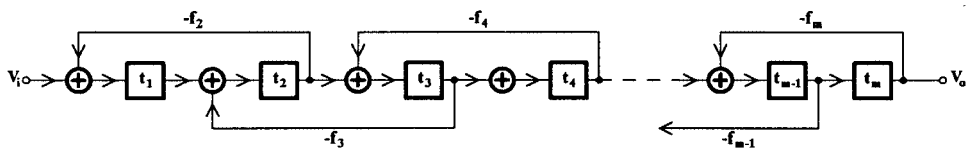

FIGURE 5.5
The leapfrog topology.

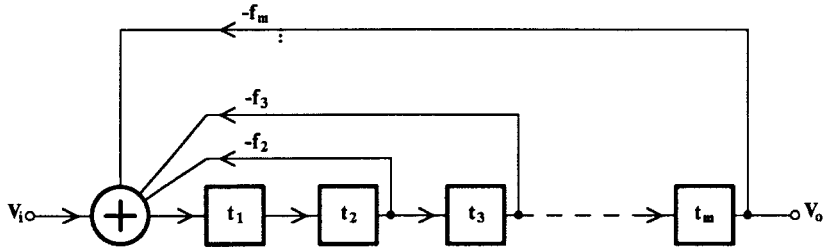

FIGURE 5.6
The summed-feedback topology.

The leapfrog topology is useful in the functional simulation of an LC ladder, and it is explained in the next chapter. The summed-feedback topology, as it appears in Fig. 5.6, is not suitable for realizing any finite transmission zeros. To overcome this problem, two useful techniques are the following:

a. The multiple- or distributed-input technique, shown in Fig. 5.7, in which the input signal is also feeding the input of all cascading sections, and
b. The summation of the input signal and the output signals from all cascaded sections, as shown in Fig. 5.8.

The topology in Fig. 5.6, and subsequently those in Figs. 5.7 and 5.8, are in fact generalizations (or adaptations) of similar analog computer methods for solving differential equations.

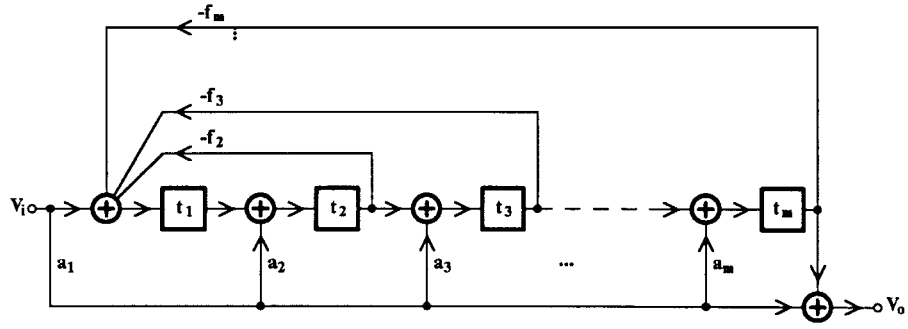

FIGURE 5.7
Summed-feedback distributed-input topology.

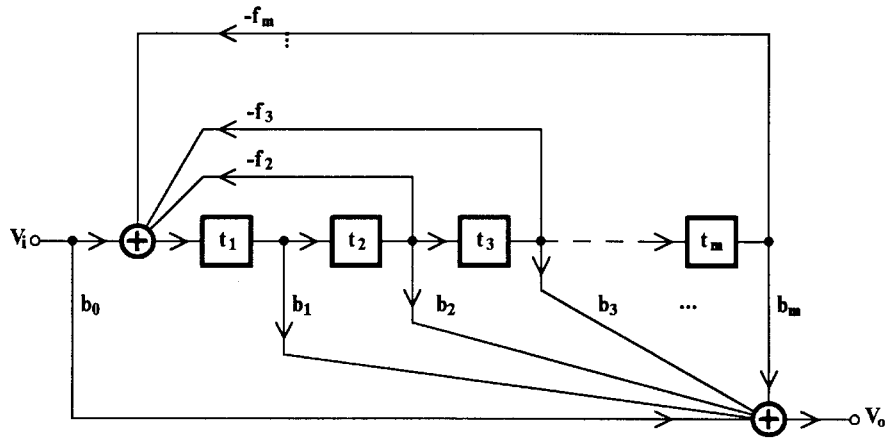

FIGURE 5.8
Summed-feedback summed-output topology.

To show this, consider for simplicity an nth-order lowpass function.

$$F(s) = \frac{K}{s^n + a_{n-1}s^{n-1} + \ldots + a_1 s + a_o} \tag{5.26}$$

This is to be realized as the voltage ratio V_o/V_i, in which case we will have, from (5.26)

$$V_o(s) = \frac{K}{s^n + a_{n-1}s^{n-1} + \ldots + a_1 s + a_o} V_i(s) \tag{5.27}$$

We can rewrite Eq. (5.27) in the following form:

$$s^n V_o = KV_i - (a_{n-1}s^{n-1} + a_{n-2}s^{n-2} + \ldots + a_1 s + a_o)V_o \tag{5.28}$$

Observe that V_o can be obtained from s^nV_o by integrating s^nV_o successively n times. If we then add KV_i and the output voltages from each integrator, weighted and signed according to Eq. (5.28), we will obtain s^nV_o. This is shown in Fig. 5.9 in block diagram form for n even. If the summation produces an extra sign reversal, the voltages should be summed with opposite signs. All voltages that take part in Eq. (5.28), with the opposite sign of that required, can have their sign reversed by summing them properly weighted, separately, using an opamp, the output of which is then connected to the input of the main summer in Fig. 5.9.

As an example, consider again the realization of the third-order Butterworth lowpass function

$$T(s) = \frac{1}{s^3 + 2s^2 + 2s + 1} = \frac{V_o(s)}{V_i(s)} \tag{5.29}$$

Writing this in the form of Eq. (5.28), we will have

$$s^3 V_o = V_i - (2s^2 + 2s + 1)V_o$$

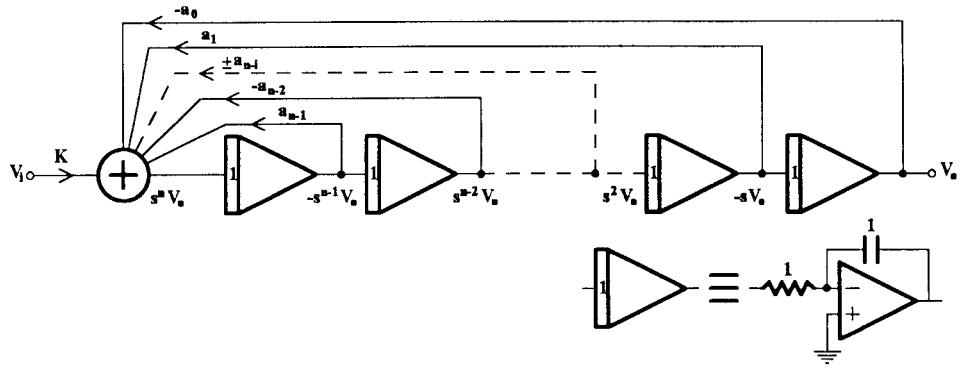

FIGURE 5.9
Realization of Eq. (5.28) using the analog computer technique. All time constants are normalized to unity.

Using single-input opamps, the complete circuit realizing the function will be as it is shown in Fig. 5.10. Notice that, from the output of the main summer, we additionally obtain the realization of the third-order Butterworth highpass function.

It can also be seen from Figs. 5.9 and 5.10 that any finite transmission zeros can be produced by summing voltages from the outputs of the various integrators properly signed and weighted. For example, the output of summer No. 2 in Fig. 5.10 gives the realization of the following function:

$$\frac{V'_o(s)}{V_i(s)} = -(2s^2+1)\frac{V_o}{V_i} = -\frac{2s^2+1}{s^3+2s^2+2s+1}$$

Three other design methods based on the topology of Fig. 5.6 have been proposed and studied. These are the following:

- The primary-resonator block (PRB) [7, 8]
- The follow-the-leader feedback (FLF) [9, 10] and
- The shifted-companion form (SCF) [11].

Both the FLF and SCF networks are generalizations of the PRB network. In what follows, we review first the SCF method, in which we include the PRB, and then the FLF design.

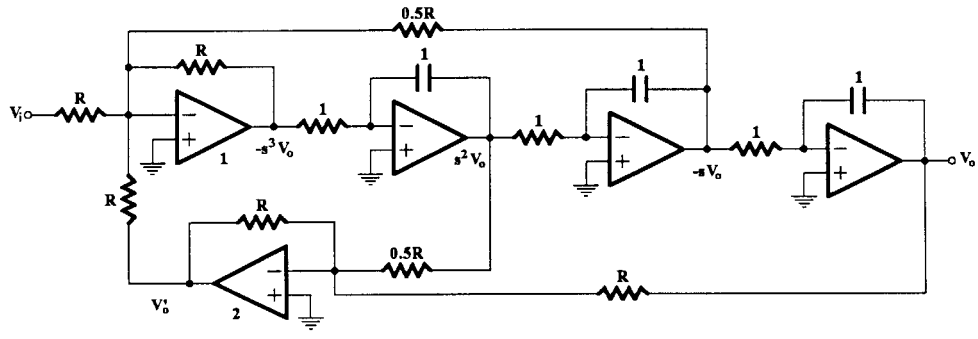

FIGURE 5.10
The analog computer approach to realizing the third-order Butterworth lowpass filter function.

5.6.1 The Shifted-Companion-Form (SCF) Design Method

For simplicity, we will explain this method by means of applying it to realize the third-order Butterworth lowpass function, Eq. (5.29). We proceed as follows.

First we select a parameter α, and we use it to shift the frequency variable s to a new frequency variable p such that

$$s = p - \alpha \tag{5.30}$$

We then introduce this into the expression for $T(s)$ Eq. (5.29) and obtain

$$T(p) = \frac{1}{(p-\alpha)^3 + 2(p-\alpha)^2 + ((p-\alpha) + 1)}$$

or

$$T(p) = \frac{1}{p^3 + a_2 p^2 + a_1 p + a_o} \tag{5.31}$$

where

$$\begin{aligned} a_2 &= 2 - 3\alpha \\ a_1 &= 3\alpha^2 - 4\alpha + 2 \\ a_o &= 1 - \alpha^3 + 2\alpha^2 - 2\alpha \end{aligned} \tag{5.32}$$

For an nth-order function, when the coefficient of p^n is 1, the usual selection of α is such that makes the coefficient of p^{n-1} equal to zero. This is, in fact, the ratio of the coefficient of s^{n-1} in the original denominator polynomial divided by n, the order of the function. In accordance with this, we get from the first of Eqs. (5.32) the following value of α:

$$\alpha = \frac{2}{3}$$

Using this in the rest of Eqs. (5.32), we get a_1 and a_o, i.e.,

$$a_1 = 2/3 \qquad a_o = 0.25926$$

Thus, $T(p)$ becomes

$$T(p) = \frac{1}{p^3 + \frac{2}{3}p + \frac{7}{27}} = \frac{1}{p^3 + 0.6667p + 0.25926} = \frac{V_o}{V_i}(p) \tag{5.33}$$

This transfer function can be realized by the block diagram (companion-form) of Fig. 5.11.

We now apply an opposite shift operation on the block diagram in Fig. 5.11 and obtain the block diagram in Fig. 5.12. Notice that, in order to obtain unity gain at dc, V_i is multiplied by $\alpha - 3$. This block diagram can be implemented in practice as shown in Fig. 5.13, assuming $C = 1$.

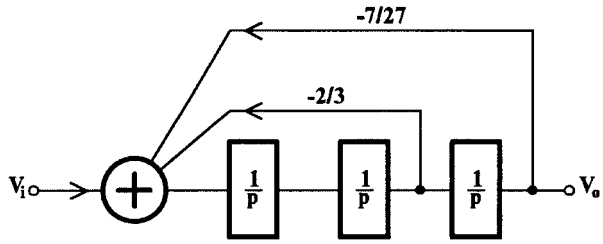

FIGURE 5.11
Realization of Eq. (5.33) in block diagram form.

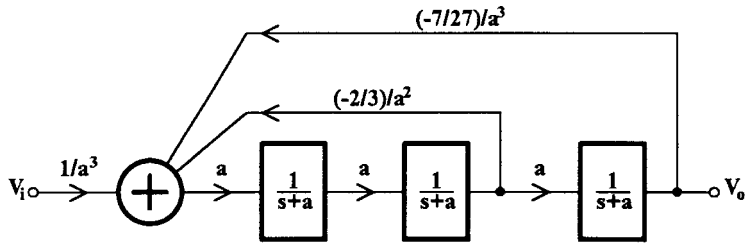

FIGURE 5.12
Realization of $T(s)$ in block diagram form.

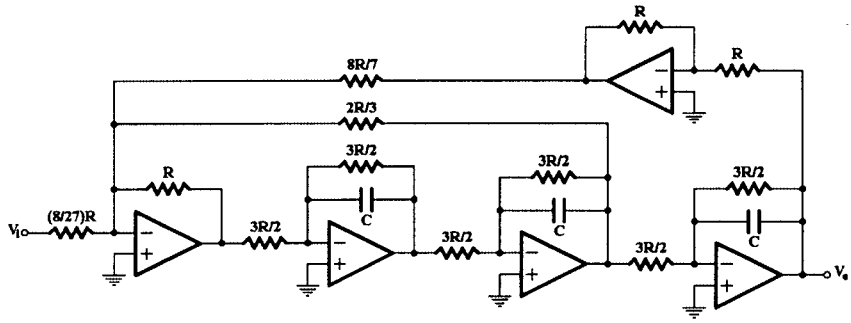

FIGURE 5.13
Final circuit realizing $T(s)$, Eq. (5.29).

A saving of one opamp (or two) in the circuit of Fig. 5.13 can be achieved if the summation of voltages, input, and feedback is performed using both inverting and noninverting inputs of the summer, or if the operation of summation is performed by the first lossy integrator with the opamp operating in differential mode.

The general SCF network has its first stage different from the others, because it performs the operation

$$\frac{1}{s + a_{n-1} + \alpha}$$

In this case, α is not selected as it was above, i.e., to make a_{n-1} equal to zero. However, when $a_{n-1} = 0$, because the value of α is selected for this purpose, the SCF network has all its stages identical, and the whole SCF circuit is identical to the PRB network.

By applying the usual lowpass-to-bandpass transformation

$$s_n = \frac{s^2 + \omega_o^2}{Bs}$$

to the block diagram in Fig. 5.12, the block diagram implementation of the geometrically, symmetric sixth-order Butterworth bandpass function will be obtained. In this case, each stage in the cascade becomes of order 2, and it requires a bandpass biquad for its realization. However, the feedback factors do not have to be changed.

Similarly, the highpass Butterworth filter function realization will be obtained if, in Fig. 5.12, the lowpass-to-highpass transformation is applied.

It should be mentioned that the PRB circuit cannot realize filters with finite transmission zeros, while the SCF can if α is not selected to make $a_{n-1} = 0$. In fact, by the general SCF network any transfer function, lowpass, highpass, bandpass, bandstop, and allpass can be realized. Of course, the summation or the feed-forward technique will be used for the realization of transmission zeros.

As a design example let us apply the transformation

$$s_n \rightarrow \frac{s^2 + 1}{0.1s}$$

as we did in the case of the CF. Then, each cascaded stage will become bandpass, as follows:

$$T(s) = \frac{\alpha}{\frac{s^2 + 1}{0.1s} + \alpha} = \frac{0.1\alpha s}{s^2 + 0.1\alpha s + 1}$$

With $\alpha = 2/3$, we finally get for $T(s)$

$$T(s) = \frac{0.0666667s}{s^2 + 0.0666667s + 1}$$

The Q factor of all stages is 15, thus the SAB in Fig. 5.3 can be used for the realization of each bandpass section, with all of these SABs being identical.

Since all three cascaded stages are tuned to the same center frequency and have equal Q factors and gains (unity), they will have the same maximum output voltage and there is no need to take any more steps to maximize the dynamic range of the filter.

Coming to the design of the SABs, we select $r = 1/49$ and, following the procedure outlined in Section 4.5, we obtain the component values, normalized and denormalized (ω_o = 1krad/s and R_o = 10 kΩ) given in Table 5.2. The overall circuit is given in Fig. 5.14(a) with each block representing the SAB in Fig. 5.14(b).

5.6.2 Follow-the-Leader Feedback Design (FLF)

The general FLF circuit is shown in block diagram form in Fig. 5.15. Clearly, the summation of the feedback voltages is responsible for the realization of the poles of the function, whereas the second summation is required for the realization of any finite transmission zeros. Here, $t_i(s)$ can be first-order lowpass or highpass functions or, alternatively, second-order functions.

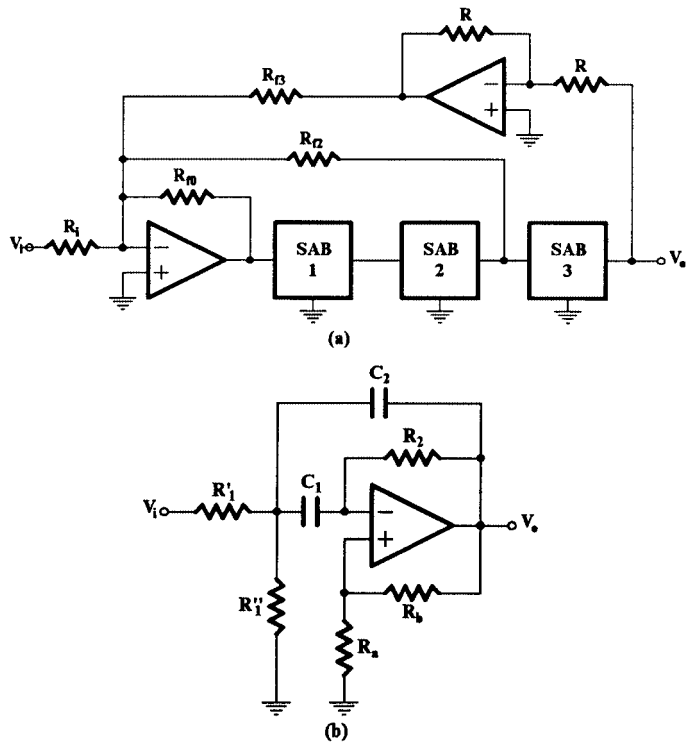

FIGURE 5.14
(a) The overall bandpass filter and (b) the circuit of each SAB.

TABLE 5.2

Component Values

	Values	
Component	**Normalized**	**Denormalized kΩ, nF**
R'_1	15.47	154.7
R''_1	0.1442	1.442
R_2	7	70
C_1	1	100
C_2	1	100
R_a	0.3129	3.129
R_b	10	100
R_i	0.296	2.96
R_{f0}	1	10
R_{f2}	0.6667	6.667
R_{f3}	1.143	11.43
R	1	10

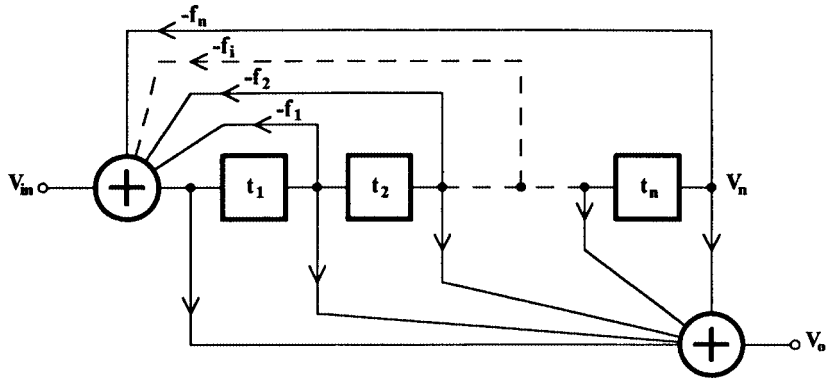

FIGURE 5.15
Block diagram of the general FLF circuit.

If we concentrate on all-pole functions the FLF block diagram can take the practical form shown in Fig. 5.16, where an opamp is used to perform the summation of the feedback voltages, assuming that there is no sign reversal in each t_i, $i = 1, 2,\ldots, n$, block.

This circuit is topologically similar to the SCF and PRB, except that there exists feedback from the output of stage t_1, which is missing in the case of the PRB circuit, although it can be considered part of the local feedback in the SCF circuit. It also differs from the PRB and the SCF circuits in that all t_i, $i = 1, 2,\ldots, n$ stages are not identical. However, it is possible to assume identical t_i and $R_1 = \infty$, in which case the FLF circuit becomes identical to the PRB circuit.

On the other hand the different t_i, $i = 1, 2,\ldots, n$ stages and the feedback from the t_1 stage can be used advantageously as additional degrees of freedom in order to improve the sensitivity of the FLF circuit. It has been shown [5], though, that this sensitivity improvement of the optimized FLF circuit is not so high as to force the designer to seek the optimized FLF circuit, if the PRB circuit can be used instead. For this reason, we do not include the optimization procedure here, but the reader can consult the relevant references [7–11] in order to satisfy any interest in the subject.

It was explained in Section 5.5 that the dynamic range is an important parameter in a high-order filter design using the cascade method. The same is true in the case of all multiple-loop feedback filters. Thus, the gain of the filter has to be properly distributed among the cascaded stages t_i so that the maximum voltage appearing at the output of each stage

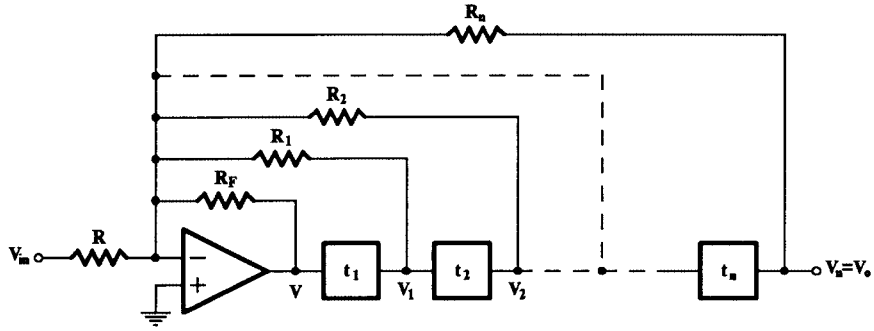

FIGURE 5.16
The practical FLF circuit with no finite transmission zeros.

is the same in all stages. The procedure to do this is the same as that followed in the cascade design, and it is not repeated here. However, we should note that in the PRB design, this gain distribution procedure is mathematically simpler than in the cascade or other FLF designs since, in the PRB design, all t_i stages are identical.

However, the optimized FLF design has been shown [12] to be the most practical multiple-loop feedback design based on sensitivity, dynamic range, and noise performance.

5.7 Cascade of Biquartics

As discussed in the previous sections, the CF filter is easy to design and tune, but its sensitivity in the passband is rather high compared to that of the MLF filters, when properly designed. MLFs, however, are difficult to adjust in practice. The cascade of biquartics filter, CBR, has been proposed [13] as an intermediate case, i.e., a filter with sensitivity in the passband lower than that of the CF filter, but which is easier to tune than the MLF filters. The design of CBR filters has been optimized [14–16] in the case of high-order geometrically symmetric bandpass filters with zeros at the origin and infinity. Therefore, here we will examine the design of this type of filters only. We refer to the stages of the CBR filter, which are of fourth order, as biquartic sections, or BR sections.

5.7.1 The BR Section

The block diagram of the BR stage is shown in Fig. 5.17. Each $t_i(s)$ stage, $i = 1, 2$, is a bandpass biquadratic function of the form

$$t_i(s) = \frac{h'_i s}{s^2 + \frac{\omega'_i}{Q'_i} s + \omega'^2_i} \tag{5.34}$$

Here, f is real and positive. If $f = 0$, the BR stage becomes the cascade of two biquadratics, which is of no interest to us here.

It should be mentioned that the topology of the BR section is the common topology of all MLF circuits, i.e., SCF, FLF, PRB, and LF, when these filters realize a fourth-order filter function. The transfer function of the BR stage is

$$T_{12}(s) = \frac{V_o}{V_i} = \frac{\alpha t_1(s) t_2(s)}{1 + f t_1(s) t_2(s)} = \alpha \frac{N(s)}{D(s)} \tag{5.35}$$

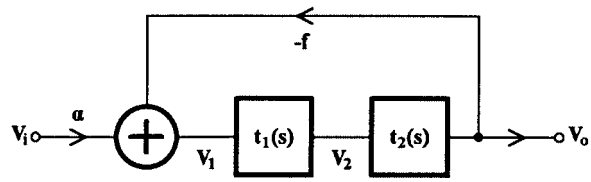

FIGURE 5.17
Block diagram of a BR section.

where $D(s)$ is a polynomial of fourth degree when $t_1(s)$ and $t_2(s)$ are given by Eq. (5.34) and

$$N(s) = h'_1 h'_2 s^2 \tag{5.36}$$

The gain coefficient is easily adjusted and can be useful to the designer in optimizing the dynamic range of the filter. We can set it equal to unity for reasons of simplicity.

Consider now the biquartic function

$$T_\alpha(s) = T_1(s) \cdot T_2(s) \tag{5.37}$$

with each $T_i(s)$, $i = 1, 2$ having the following form:

$$T_i(s) = \frac{h_i s}{s^2 + \frac{\omega_i}{Q_i} s + \omega_i^2} \tag{5.38}$$

If $T_\alpha(s)$ is to be realized by the biquartic section in Fig. 5.17, $D(s)$ in Eq. (5.35) has to be identified by the denominator of $T_\alpha(s)$ and similarly for $N(s)$. Thus, $D(s)$ will be

$$D(s) = \left(s^2 + \frac{\omega_1}{Q_1} s + \omega_1^2\right)\left(s^2 + \frac{\omega_2}{Q_2} s + \omega_2^2\right) \tag{5.39}$$

But from Eqs. (5.35) and (5.34), $D(s)$ is also given by

$$D(s) = \left(s^2 + \frac{\omega'_1}{Q'_1} s + \omega'^2_1\right)\left(s^2 + \frac{\omega'_2}{Q'_2} s + \omega'^2_2\right) + f h'_1 h'_2 s^2 \tag{5.40}$$

or

$$D(s) = D'(s) + \eta s^2 \tag{5.41}$$

where

$$D'(s) = \left(s^2 + \frac{\omega'_1}{Q'_1} s + \omega'^2_1\right)\left(s^2 + \frac{\omega'_2}{Q'_2} s + \omega'^2_2\right) \tag{5.42}$$

and

$$\eta = f h'_1 h'_2 \tag{5.43}$$

with η set in this form for convenience. Notice that $\eta > 0$.

Our task now is to determine $D'(s)$ and η (and consequently f) for the biquartic to realize $T_\alpha(s)$ in Eq. (5.37).

5.7.2 Effect of η on ω'_i and Q'_i

From Eqs. (5.41), (5.39), and (5.40), using simple algebra, the following equations can be obtained:

$$\frac{\omega'_1}{Q'_1} + \frac{\omega'_2}{Q'_2} = \frac{\omega_1}{Q_1} + \frac{\omega_2}{Q_2} \tag{5.44}$$

$$\omega'^2_1 + \omega'^2_2 + \frac{\omega'_1\omega'_2}{Q'_1Q'_2} = \omega_1^2 + \omega_2^2 + \frac{\omega_1\omega_2}{Q_1Q_2} - \eta \tag{5.45}$$

$$\frac{\omega'_1}{Q'_2} + \frac{\omega'_2}{Q'_1} = \frac{\omega_1}{Q_2} + \frac{\omega_2}{Q_1} \tag{5.46}$$

$$\omega'_1\omega'_2 = \omega_1\omega_2 \tag{5.47}$$

In the case of geometrically symmetric bandpass filters which have been obtained from the transformation of an all-pole lowpass function to bandpass, each pair of complex conjugate poles of the lowpass function transforms to two pairs of poles of the bandpass function which have identical Q factors.

Thus, depending on which two pairs of poles of the bandpass function the BR section is to realize, we distinguish two cases when referring to Eqs. (5.44) through (5.47).

a. $Q_1 = Q_2 = Q$ (symmetrical stage)
b. $Q_1 \neq Q_2$ (nonsymmetrical stage)

It has been shown [16] that the symmetrical stage is more advantageous in practice than the nonsymmetrical one. This will be explained later, when the realization of the overall function will be considered. Thus, the nonsymmetrical case will not be considered further here.

Referring to the symmetrical stage then, substituting Q for Q_1 and Q_2 in Eqs. (5.44) and (5.46) gives

$$\frac{\omega'_1}{Q'_1} + \frac{\omega'_2}{Q'_2} = \frac{\omega_1 + \omega_2}{Q} \tag{5.48}$$

and

$$\frac{\omega'_1}{Q'_2} + \frac{\omega'_2}{Q'_1} = \frac{\omega_1 + \omega_2}{Q} \tag{5.49}$$

Subtracting (5.49) from (5.48) or vice-versa and after some manipulation the following is obtained:

$$\left(\frac{1}{Q'_1} - \frac{1}{Q'_2}\right)(\omega'_1 - \omega'_2) = 0 \tag{5.50}$$

which gives the relationship between Q'_i and ω'_i, $i = 1, 2$.

Clearly, the values of Q'_i and ω'_i, $i = 1, 2$, will depend on the value of η as a consequence of Eq. (5.45). It can then be observed by means of Eq. (5.50), that there is a range of values of η for which

$$\omega'_1 = \omega'_2 \qquad Q'_1 \neq Q'_2$$

and another range of η values for which

$$\omega'_1 \neq \omega'_2 \qquad Q'_1 = Q'_2$$

and, finally, a value of $\eta = \eta_o$ for which

$$\omega'_1 = \omega'_2 \qquad Q'_1 = Q'_2$$

These can be clearly illustrated by means of an example. Consider pairing the equal Q factor biquadratics $T_b(s)$ and $T_c(s)$ of $T(s)$, Eq. (5.22), in order to form the biquartic function of interest here. In this case (however, see design example below with different indices)

$$Q_1 = Q_2 = Q = 20.0187$$

$$\omega_1 = 0.9576228$$

$$\omega_2 = 1.0442525$$

Using these values in Eqs. (5.45), (5.47), (5.48), and (5.49) the two diagrams in Fig. (5.18) can be obtained.

The value of $\eta = \eta_o$ is most interesting, because the two biquadratics $t_1(s)$ and $t_2(s)$ become identical and, consequently, the corresponding stages in the BR will be identical. This can be the starting point in any CBR filter design as it is considered here. We can determine this value η_o from Eq. (5.45) as follows.

Since, for identical $t_1(s)$ and $t_2(s)$,

$$\omega'_1 = \omega'_2 = \omega' \qquad Q'_1 = Q'_2 = Q'$$

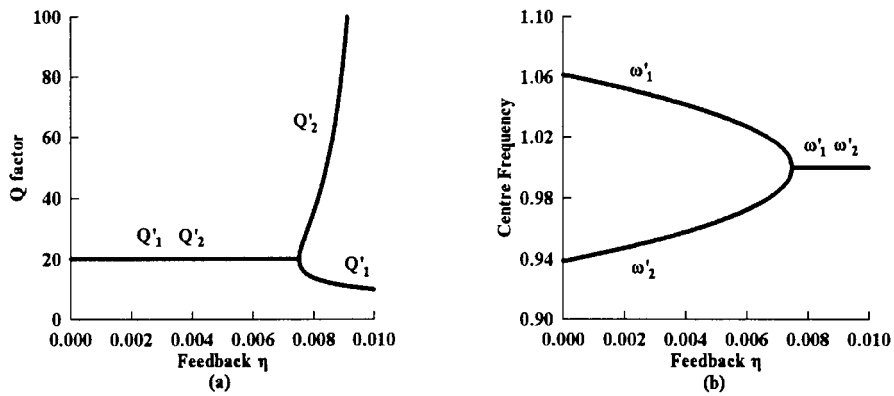

FIGURE 5.18
Effect of varying η on (a) the Q factors Q'_i and (b) the center frequencies ω'_i, i = 1,2 of biquads $t_1(s)$, $t_2(s)$, symmetrical stage.

substituting in Eq. (5.47) gives

$$\omega' = \sqrt{\omega_1 \omega_2} \tag{5.51}$$

Also from Eq. (5.48) using (5.51)

$$Q' = Q\frac{2\sqrt{\omega_1 \omega_2}}{\omega_1 + \omega_2} \tag{5.52}$$

Then, inserting these values in Eq. (5.45), the following value of η is obtained:

$$\eta = \eta_o = (\omega_1 - \omega_2)^2\left(1 - \frac{1}{4Q^2}\right) \tag{5.53}$$

5.7.3 Cascading Biquartic Sections

Biquartic sections can be cascaded to realize high-order filter functions. There is no need for isolation stages between the BR sections, since their outputs are of low impedance, being the output of an opamp with negative voltage feedback. Thus, the cascade of biquartic sections filter or CBR filter is obtained.

As mentioned above, we consider here the realization of bandpass filter functions, which have been obtained from an all-pole lowpass via the usual lowpass-to-bandpass transformation. These functions will be of the following form:

$$T(s) = \prod_{i=1}^{N} T_i(s) \tag{5.54}$$

where each $T_i(s)$ will be given by Eq. (5.38).

Thus, the order of $T(s)$ will be $2N$, with N being even or odd.

If N is even, $T(s)$ can be written as the product of biquartic functions, each of them having in their numerator only a s^2 term multiplied by a constant. On the other hand, if N is odd, one bandpass biquadratic term can be separated from $T(s)$ and realized separately. Then, the rest of $T(s)$ will be of an order divisible by 4 and therefore will be treated as when N is even.

For an optimum CBR filter design, various degrees of freedom should be considered, namely, pairing the pole-pairs to obtain the biquartics, position of each BR section in the cascade, and distribution of the overall gain among the various stages. These degrees of freedom are to be considered in this and following sections.

Pairing pole pairs for obtaining symmetrical BR sections, apart from being practically more desirable than the nonsymmetrical sections, leads to further advantages [16] concerning sensitivity and noise. There is not much difference between the two cases, as far as dynamic range is concerned. Following this reasoning, pole-pairs are preferably paired in a way that symmetrical BR sections will be obtained.

5.7.4 Realization of Biquartic Sections

There is a flexibility in the realization of each biquartic section (Fig. 5.17), depending on the Q factor of the biquadratic blocks, t_i [Eq. (5.34)]. Thus, for Q factors ≤ 30 and in the audio

frequencies regime, SABs [17] can be used [18] in the realization. Then, the overall BR section will be as shown in Fig. 5.19(a). However, since the possibility exists with this SAB to use both inputs of the operational amplifier to obtain summation of voltages, the summer can be eliminated, and the BR circuit will be as shown in Fig. 5.19(b) using two operational amplifiers.

In BR sections, in which the Q factors of the biquadratic blocks are greater than 30, two-opamp or even three-opamp biquads should be used. A suitable two-opamp biquad is the GIC-type biquad [19] shown in Fig. 5.20, which will take the place of each SAB in Fig. 5.19(a).

The two biquads, SAB and GIC-type, have been studied [20–22] and optimized from the sensitivity and noise points of view and, for this reason, they are used in the realization of filter functions here.

5.7.4.1 Design Example

For reasons of comparison, let us consider the use of this technique to design the sixth-order Butterworth bandpass filter that we have also designed as a CF and a PRB (SCF) filter.

Since it is a sixth-order function, we choose to pair the two equal-Q pole biquadratics in order to form the BR function, while the remaining lower-Q second-order bandpass function will be realized by the SAB in Fig. 5.3. Thus, we will have, from Eq. (5.22)

$$T_2(s)T_3(s) = \frac{k_2\ 0.047832s}{s^2 + 0.0478362s + 0.9170415} \times \frac{k_3\ 0.0521638s}{s^2 + 0.521638s + 1.0904632}$$

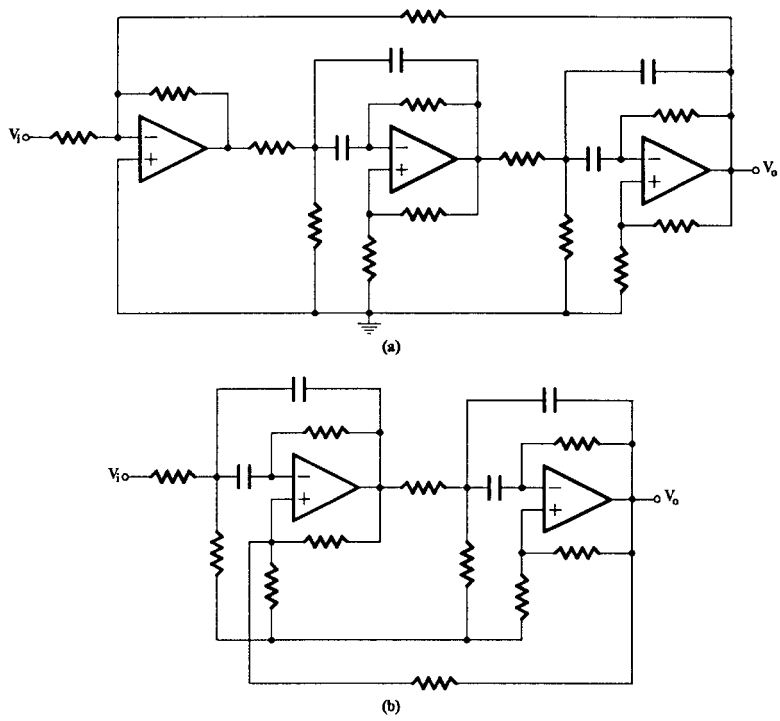

FIGURE 5.19
Realization of a BR section using (a) three and (b) two operational amplifiers.

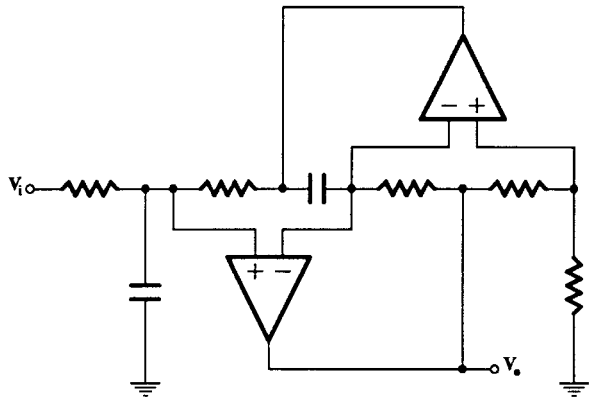

FIGURE 5.20
GIC-type biquad.

with

$$\omega_2 = 0.9576228 \qquad Q_2,\ Q_3 = 20.0187 = Q$$

$$\omega_3 = 1.0442525$$

and

$$D(s) = s^4 + 0.1s^3 + 2s^2 + 0.11s + 1$$

Then,

$$\omega'_2 = \omega'_3 = \sqrt{\omega_2\omega_3} = 1$$

$$Q'_2 = Q'_3 = \frac{2\sqrt{\omega_2\omega_3}}{\omega_2 + \omega_3}Q = \frac{2 \times 20.0187}{2.0018753} = 20.00$$

and

$$\eta_o = (\omega_2 - \omega_3)^2\left(1 - \frac{1}{4Q^2}\right) = 0.0075$$

It can be seen that Q'_2, Q'_3 are slightly less than Q, while the two biquads in the BR stage will be tuned to the center frequency of the filter. Then,

$$t_2(s) = t_3(s) = \frac{0.04999689s}{s^2 + 0.04999689s + 1}$$

In practice it will be impossible to realize the coefficient of s using components even of 0.1 percent tolerance. So, to a very good approximation, we can write this function practically as follows:

$$t_2(s) = t_3(s) = \frac{0.05s}{s^2 + 0.05s + 1}$$

Two identical SABs will be used to realize $t_2(s)$ and $t_3(s)$.

To complete the design, we must calculate the feedback ratio f using the value of η_o. From Eq. (5.43), we will have

$$f = \frac{\eta_o}{h'_2 h'_3} = \frac{0.0075}{0.05 \times 0.05} = 3$$

If we choose to have the biquad (SAB) leading in the cascade, the overall filter will be as shown in Fig. 5.21 in block diagram form. The summation is performed using an opamp as is shown in Fig. 5.22.

Component values for the overall filter are given in Table 5.3, both normalized, and denormalized to $R_o = 10\ \text{k}\Omega$ and $\omega_o = 1\text{krad/s}$.

5.7.5 Sensitivity of CBR Filters

Having dealt with the problem of realization of the CBR filters, we can now proceed to examine their sensitivity and, if possible, optimize their design from this point of view. It is clear that the filter sensitivity will not depend on the sequence of the BR sections in the cascade. It will, however, depend on the feedback ratios η, on the types and the design of biquads used, and on the particular pairing of pole pairs to form the biquartic functions.

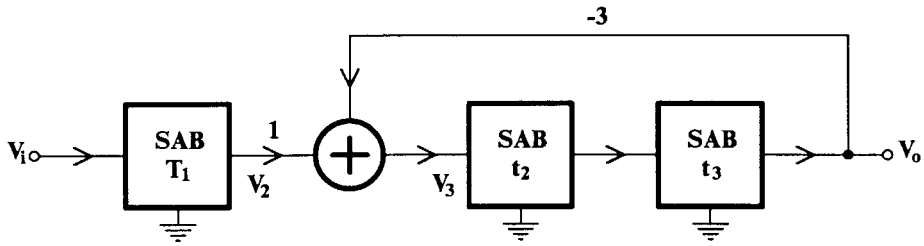

FIGURE 5.21
Realization of $F(s)$ using a SAB and a BR section connected in cascade. SABs t_2 and t_3 are identical.

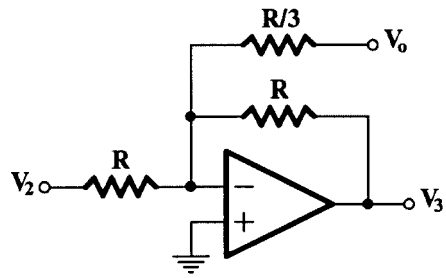

FIGURE 5.22
Opamp for performing summation.

TABLE 5.3

Component Values

	SAB T_1		SABs t_2, t_3	
Component	Normalized	Denormalized kΩ, nF	Normalized	Denormalized kΩ, nF
R'_1	10.27	102.7	20.67	206.7
R''_1	0.145	1.45	0.1439	1.44
R_2	7	70	7	70
C_1	1	100	1	100
C_2	1	100	1	100
R_a	0.265	2.65	0.33678	3.37
R_b	10	100	10	100
R	–	–	1	10

The sensitivity of the CBR circuit has been examined [16] realizing an eighth-order, 0.5 dB ripple Chebyshev bandpass filter function, which has been obtained from the corresponding all-pole lowpass via the transformation

$$s_n = \frac{s^2 + 1}{0.1s}$$

The standard deviation of the magnitude response of the filter was considered as the sensitivity measure. This was calculated according to a Monte Carlo method for 1000 tries. All passive components were assumed to have values uniformly distributed within their tolerance limits ±1 percent, and operational amplifiers were assumed to correspond to one-pole model with 10 percent tolerance in their gain-bandwidth product ($f_T = 1$ MHz). Results are as follows.

The sensitivity is reduced as the feedback ratio η increases up to the η_o value. Further increase in $\eta > \eta_o$ does not lead to substantial further reduction in sensitivity. It appears that sensitivity reduction of the BR section as η increases follows the reduction in the difference $\omega'_1 - \omega'_2$ and becomes nearly constant when $\omega'_1 = \omega'_2$ for $\eta \geq \eta_o$. In all cases ($0 < \eta < \eta_{max}$), the sensitivity of the BR section is lower than the sensitivity of this section with $f = 0$ (cascade filter). Here, by η_{max}, the value of η is denoted for which one of the Q'_i factors becomes infinite. This value can be obtained from Eq. (5.45) for the symmetrical case to be

$$\eta_{max} = (\omega_1 - \omega_2)^2 + \frac{\omega_1 \omega_2}{Q^2} \tag{5.55}$$

SABs can be used instead of GIC-type biquads, if the Q factors of the biquadratics in a BR stage are low (≤30), thus saving in operational amplifiers. It has been shown in this case [16] that the two CBR circuits are equivalent from the sensitivity point of view, but in the circuits with SABs, there is a saving of at least two operational amplifiers. Also, noise performance should be superior since, as has been shown [15], CBR circuits with SABs are less noisy than CBR circuits with GIC-type biquads.

Referring to the position of each BR section in the cascade, it has been shown [15, 16] that, as a rule of thumb, the BR sections should be placed in ascending Q factor order starting with the lowest Q section. This result is in agreement with the optimum ordering in the CF case.

5.8 Summary

The realization of a high-order filter function is necessary when the designer's filter problem is to satisfy the stringent selectivity requirements in telecommunication systems, special instrumentation and many other applications. Direct methods of realization of such filter functions using only one opamp are not practical, because they result in highly sensitive active circuits.

In this chapter, three practical methods of realizing high-order filter functions have been reviewed. A fourth method is explained in the next chapter. The three methods, namely, the cascade connection of second-order stages, CF; the multiple-loop feedback, MLF; and the cascade connection of fourth-order stages, CBR, have advantages and disadvantages. Thus, the CF can realize any type of stable filter function, is easy to design and tune, and requires fewer opamps than the other filters. Its disadvantage is the higher sensitivity in the passband compared to the other filters.

Three MLF circuits were reviewed. The primary-resonator block, the follow-the-leader feedback, and the shifted-companion form. Their common characteristic is the application of negative feedback in a cascade connection of low-order stages, first- or second-order, depending on the type of filter function, whether it is lowpass (highpass) or bandpass (bandstop), respectively. The MLF circuits have low sensitivity in the passband—much lower than the CF—but their design and tuning are more involved than in the case of the corresponding CF. The SCF is the most general of the three, while the FLF can be optimized to have lowest sensitivity and noise. The PRB is practically suitable for the realization of geometrically symmetric bandpass filters when the design of the SCF and the nonoptimized FLF result in the same PRB circuit.

The cascade connection of biquartic stages, CBR, is an alternative and useful approach for the design of geometrically symmetric bandpass filters. It combines the advantages of the CF (easy to design and tune) with the low sensitivity characteristics of the MLF. It has been proven also to display noise performance similar to that of the FLF circuit, which is the best among all the MLF circuits. Lowpass active filters of special form [23] as well as other filter functions [13, 24] can also be realized as CBR circuits, but the optimization procedure outlined above was derived [15] for the case of the geometrically symmetric bandpass filters only.

From the previous discussion, one can conclude that, when the selectivity demand is relatively low, the CF can be the preferable solution. However, when this demand is more stringent, the PRB or the CBR filters should be the choice provided, of course, that they can realize the pertinent function. Otherwise, the designer should look for an optimized FLF circuit or for a LC ladder simulated circuit provided, of course, that a suitable LC ladder realizing the required transfer function exists.

The method of LC ladder simulation leads to active RC filters of very low sensitivity,—lower than that of the MLF circuits—and is examined in the following two chapters.

References

[1] J. D. Schoeffler. 1976. "The synthesis of minimum sensitivity networks," *IEEE Trans. Circuit Theory* CT-11, 272–276.

[2] I. M. Sobel. 1975. *The Monte-Carlo Method,* Moscow: Mir Publishers, Moscow.
[3] G. S. Moschytz. 1975. *Linear Integrated Networks: Design,* New York: Van Nostrand-Reinhold.
[4] E. Lueder. 1970. "A decomposition of a transfer function minimization distortion and in band losses," *Bell Syst. Tech. J.* **49**, pp. 455–569.
[5] A. S. Sedra and P. O. Bracket. 1978. *Filter Theory and Design: Active and Passive,* London: Pitman.
[6] S. Halfin. 1970. "An optimization method for cascaded filters," *Bell Syst. Tech. J.* **44**, pp. 185–190.
[7] G. Hurtig, III. 1972. "The primary resonator block techniques of filter synthesis," *Proc. Int. Filter Symposium,* p. 84.
[8] G. Hurtig, III. 1973. Filter network having negative feedback loops, U.S. patent B, 720,881.
[9] K. R. Laker and M. S. Gausi. 1974. "Synthesis of a low sensitivity multiloop feedback active RC filter," *IEEE Trans. Circuit and Systems* CAS-21, pp. 252–259.
[10] *ibid*. 1974. "A comparison of active multiple-loop feedback techniques for realising high order bandpass filters," pp. 774–783.
[11] J. Tow. 1975. "Design and evaluation of shifted companion form active filters," *Bell Syst. Tech. J.* **54**, pp. 545–568.
[12] C. F. Chiou and R. Schaumann. 1980. "Comparison of dynamic range properties of high-order active bandpass filters," *Proc. IEEE* **127**, Pt, G, pp. 101–108.
[13] J. Tow. 1978. "Some results on two-section generalized FLF active filters," *IEEE Trans. Circuits and Systems,* 181–184.
[14] T. Deliyannis and S. Fotopoulos. 1981. "Noise in the cascade of biquartic section filter," *Proc. IEE* **128**, Pt G,192–194.
[15] T. Deliyannis and S. Fotopoulos. 1982. "Sensitivity and noise considerations in the cascade of biquartic sections filters," *Proc. 1982 Intl. Symposium on Circuits and Systems,* ISCAS 82, Rome, 1102–1105.
[16] S. Fotopoulos and T. Deliyannis. 1984. "Active RC realisation of high order bandpass filter functions by cascading biquartic sections," *Int. J. Circuit theory and Applications* **12**, pp. 223–238.
[17] T. Deliyannis. 1968. "High Q factor circuit with reduced sensitivity," *Electron. Lett.* **4**, 577–579.
[18] P. E. Fleischer. 1976. "Sensitivity minimization in a single amplifier biquad circuit," *IEEE Trans. Circuits and Systems* CAS-23, 45–55.
[19] B. B. Bhattacharyya, W. S. Mikhael, and A. Antoniou. 1974. "Design of RC active networks using generalised-immitance converters," *J. Frank. Inst.* **297**(1), pp. 45–48.
[20] A. S. Sedra and J. L. Espinoza. 1975. "Sensitivity and frequency limitations of biquadratic active filters," *IEEE Trans. Circuits and Systems* CAS-22, 122–130.
[21] H. J. Bachler and W. Guggenbuhl. 1979. "Noise and sensitivity optimization of a single amplifier biquad," *IEEE Trans. Circuits and Systems* CAS-26, 30–36.
[22] C. F. Chiou and R. Schaumann. 1981. "Performance of GIC-derived active RC biquads with variable gain," *Proc. IEE* **128**, Pt G, pp. 46–52.
[23] M. Biey. 1983. "Design of lowpass two-section generalised FLF active filters," *Electron. Lett.* **19**, 639–640.
[24] A. N. Gonuleren. 1982. "Multiloop feedback unsymmetrical active filters using quads," *Intl. J. Cir. Theor. Appl.* **10**, 1–18.

Further Reading

R. Schaumann, M.S. Ghausi, and K.R. Laker. 1990. *Design of Analog Filters: Passive RC, and Switched Capacitor,* Englewood Cliffs, NJ: Prentice-Hall.